Available online at www.sciencedirect.com
ScienceDirect
Journal of Non-Crystalline Solids 353 (2007) 974–980
JOURNAL OF NON-CRYSTALLINE SOLIDS
www.elsevier.com/locate/jnoncrysol

Kinetics and binding properties of cloramphenicol imprinted polymers

E. Corton [a], J.A. García-Calzón [b], M.E. Díaz-García [b,*]

[a] Department of Biological Chemistry, University of Buenos Aires, Argentina
[b] Department of Physical and Analytical Chemistry, University of Oviedo, Av. Julián Clavería, 8, 33006 Oviedo, Spain

Available online 15 February 2007

Abstract

Molecularly imprinted polymers (MIPs) are easily obtained by a non-covalent approach through the copolymerisation of suitable functional monomers and cross-linkers in the presence of the print molecule. Removal of the template leaves a polymer that selectively recognises it. However, experimental data have demonstrated that non-covalent molecularly imprinted polymers exhibit a heterogeneous binding sites distribution. In this work, two different imprinted polymers for chloramphenicol (CAP), obtained using different template concentrations, were evaluated for their kinetics and affinity binding properties against CAP in a batch approach. Experimental binding isotherms were fitted to Langmuir, Freundlich and Langmuir–Freundlich isotherms and the affinity distribution corresponding to the Freundlich isotherm was used to extract binding parameters. Parallel studies were performed for the binding of chloramphenicol diacetate to the CAP-imprinted polymers.

PACS: 81.05.−t; 81.07.Nb; 81.16.Be; 81.20.Fw

Keywords: Pharmaceuticals; Polymers and organics; Adsorption

1. Introduction

In the analytical chemistry area, molecular imprinting is receiving extraordinary attention because this methodology provides an approach to synthesizing highly substrate selective polymers with applications as HPLC stationary phases for chiral resolution, in sensor design and as substitutes for biological receptors in affinity assays. The concept behind the conventional model for non-covalently imprinted polymers assumes that in solution the analyte (the template) is surrounded by functional monomers or precursors forming aggregates or complexes that are locked, during polymerisation, into the bulk polymer matrix. Upon extraction, internal images with specific binding sites for the template are left within the imprinted polymer. This non-covalent process has been demonstrated not only for organic-based (e.g. acrylic-, methacrylic-based) materials but also for inorganic ones (e.g. Si-, Ti-sol–gels).

Although the imprinting concept may predict homogeneous binding sites, experimental data have demonstrated that non-covalent molecularly imprinted polymers exhibit a heterogeneous binding sites distribution. Several reasons have been suggested for presence of heterogeneous binding sites in MIPs: (a) the amorphous nature of the polymer matrix, (b) stepwise complexation between the template and the functional monomers in solution, resulting in various structures of the pre-polymerisation complexes which will form binding sites with different affinity constants, (c) incomplete removal of template during MIP cleaning, (d) binding sites collapsing by template solvent extraction, (e) non-specific binding sites [1,2]. Although the heterogeneity of binding sites is one of the key factors that influences the performance of MIPs in its particular field of application, the study of the binding site heterogeneity in MIPs has only

* Corresponding author. Tel.: +34 985 103471; fax: +34 985 103125.
E-mail address: medg@uniovi.es (M.E. Díaz-García).

0022-3093/$ - see front matter © 2007 Elsevier B.V. All rights reserved.
doi:10.1016/j.jnoncrysol.2006.12.066

recently been addressed, particularly by the groups leaded by Shimizu et al. [3–9] and Guiochon et al. [10–26].

The preparation of a non-covalent methacrylate–vinylpyridine-based imprinted polymer for chloramphenicol (CAP) and its use as recognition phase in a fluorescent competitive flow assay has been previously reported by our group [27]. In order to understand the basis for optimisation of non-covalent molecular imprinting, in this paper two CAP imprinted polymers were prepared in presence of different CAP concentration and their kinetics and equilibrium binding properties have been evaluated using a batch rebinding approach. Similar studies were performed with these polymers for binding a CAP-related molecule, chloramphenicol diacetate (CAPdi). Experimental binding isotherms were fitted to Langmuir, Freundlich and Langmuir–Freundlich isotherms. The affinity distribution corresponding to the Freundlich isotherm was used to extract binding parameters for both CAP and CAPdi, using the two CAP- imprinted polymers. Results demonstrated the importance of the amount of template during polymer preparation for tuning the affinity of the binding process.

2. Experimental

2.1. Materials

Unless otherwise stated, chemicals were commercially available (Aldrich–Sigma Company) and used without further purification. Solvents used in the polymer preparations (THF, methanol) were obtained from Prolabo and/or Rectapur and used as received. AIBN was obtained from Fluka. UV measurements were taken on a Perkin–Elmer Lambda 900 Spectrophotometer.

2.2. General polymer synthesis

Methacrylic polymers imprinted with chloramphenicol were prepared according to a standard method by using a mixture of diethylaminoethylmethacrylate (DAM, 105 μL) and vinylpyridine (VP, 165 μL) as functional monomers, ethylene glycol dimethacrylate (EGDMA, 900 μL) as cross-linking agent and THF (3.83 μL) as the porogen. In the synthesis of MIP1, 323 mg of CAP were used, while 32 mg CAP were employed in the synthesis of MIP2. The template-monomer mixture and solvent were transferred to a test tube and α,α-azo-bis-isobutyronitrile (AIBN, 100 mg) was added. The mixture was degassed by bubbling N_2 for 10 min. The tube was sealed and heated in a block heater at 60 °C for 24 h. The control blank polymers (NIPs) were prepared using an identical procedure but in absence of the template. The polymers were obtained as brittle solids which were broken up, grounded in a mortar and sieved to an average particle size of 80–200 μm. The grounded polymers were washed to remove CAP with methanol in a soxhlet apparatus for 12–18 h and finally dried at 35 °C.

2.3. Batch binding experiments

The required mass of washed polymer (30 mg) was weighed into a 2 mL screw-cap vial. A THF solution of CAP (40 ppm) was added and the vial was sealed and gently shaked. Except in the kinetic experiments, samples were shaken for 80 min at room temperature which is more than sufficient time to allow the equilibrium binding to be established. Similar equilibrium binding experiments were performed with CAPdi to determine its binding to the polymer. The left out concentrations of CAP and CAPdi in the supernatant solutions were analyzed using UV spectrophotometer ($\lambda_{abs} = 280$ nm for CAP and $\lambda_{abs} = 266$ nm for CAPdi from individual calibrations).

2.4. Kinetic measurements

In order to demonstrate the reversible nature of the binding to the CAP-imprinted polymers a series of kinetic measurements were undertaken. Cleaned polymers were allowed to bind CAP (or CAPdi) from a 40 ppm solution. The progress of the adsorption during the experiments was determined, after desired contact time, by analysing spectrophotometrically at 280 nm for CAP (or CAPdi) concentration.

2.5. Sorption isotherms

The sorption capacity and equilibrium isotherms for CAP and CAPdi onto CAP-imprinted polymers were estimated using three equilibrium models: Freundlich (F), Langmuir (L) and Langmuir–Freundlich (L–F) isotherms.

2.5.1. Freundlich isotherm

The Freundlich isotherm is an empirical power function for non-ideal sorption on heterogeneous surfaces as well as for multilayer sorption and is expressed by the equation:

$$B = aC^m, \tag{1}$$

where B is the amount of adsorbed CAP (or CAPdi) at equilibrium, a is a Freundlich adsorption coefficient (related with the sorption capacity, N_t, and the average affinity, K_0), m is a Freundlich constant which represents the heterogeneity index and varies from zero to one (values approaching to zero indicate increasingly heterogeneity and one being homogeneous), C is the equilibrium concentration of template. The term B in Eq. (1) was calculated from the simple mass balance equation as follows:

$$B = V\frac{C_0 - C}{M}, \tag{2}$$

where C_0 is the initial CAP concentration, C is the CAP concentration at equilibrium, V is the volume of solution and M is the mass of imprinted polymer. The linearized form of Eq. (1) was obtained by taking log on both sides:

$$\log B = \log a + m \log C. \tag{3}$$

Therefore, the plot of log$B$ vs log$C$ was employed to generate the intercept value of a and the slope of m. The Freundlich equation has been derived by assuming an expo- nentially decaying sorption site energy distribution.

2.5.2. Langmuir isotherm

The Langmuir sorption isotherm assumes that adsorption takes place at specific homogeneous sites within the material. The isotherm equation is derived from simple mass action kinetics, assuming chemisorption. Also, it assumes that once a template occupies a site, no further sorption can take place at that site, that all sites are energetically equivalent and there is no interaction between molecules adsorbed on neighbouring sites. Theoretically, the imprinted polymer has a finite capacity for the template. Therefore, a saturation value should be reached beyond which no further sorption can take place. While the Langmuir model assumes that there is only a single class of binding sites, the bi-Langmuir model assumes that there are two classes of sites within the imprinted material. It is straightforward to implement the Langmuir and bi-Langmuir models using Scatchard plots to determine the binding parameters, the binding affinity (K) and the number of binding sites (N_t), using the general expression:

$$\frac{B}{C} = KN_t - KB, \tag{4}$$

where B is the amount of adsorbed CAP at equilibrium, N_t is the total number of accessible adsorption sites, C is the equilibrium concentration of template, and K is the Langmuir isotherm equilibrium constant. In homogeneous systems with only one type of binding sites, by plotting B/C against B it is possible to obtain the value of N from the x-intercept and the value of K from the slope. In heterogeneous systems, Scatchard plots are not linear and the simplest model in this case is a material with two different kinds of adsorption sites. Langmuir equation is then extended to an equation with two Langmuir terms (bi-Langmuir equation):

$$B = \frac{N_1 K_1 C}{1 + K_1 C} + \frac{N_2 K_2 C}{1 + K_2 C}. \tag{5}$$

Thus, the plot B/C vs B is composed of two straight lines, from which two sets of binding parameters (K_1,N_1 and K_2, N_2) for the two classes of binding sites within the imprinted polymer can be obtained. The steeper line corresponds to the high-affinity sites while the flatter line measured the low-affinity ones.

2.5.3. Langmuir–freundlich isotherm

This model, first described by Sips [28,29] was introduced for the MIPs by the groups of Shimizu et al. [4,5,8] and Guiochon et al. [10,13,15]. The model describes an equilibrium relationship between the concentration of a bound template (B) and the equilibrium template concentration in solution (C) such that:

$$B = \frac{N_t K_0^m C^m}{1 + K_0^m C^m}, \tag{6}$$

where N_t is the total number of binding sites and K_0 is the median binding affinity. The variable a is related to K_0 via $K_0 = a^{1/m}$. The fitting parameter, m, is identical to the heterogeneity index of site energies from the F isotherm. The difference between the L–F model and the Freundlich one is evident at high sorbate concentrations, for which the L–F model is able to represent the saturation behavior. At low sorbate concentrations the L–F equation reduces to the classical F equation. On the other hand, as m approaches unity, indicative of a completely homogeneous sorbent surface (i.e. energetic equivalence of all binding sites) the L–F equation reduces to the classical L equation. Thus, the hybridised L–F isotherm is able to model adsorption of solutes at high and low concentrations onto homogeneous and heterogeneous MIPs. Although a linear analysis is not possible for a three-parameter isotherm, the L–F isotherm can be fitted to the experimental data following the method of Shimizu et al. [4,5] in which a solver function may be used to maximize the coefficient of determination (R^2) by iteratively varying the three fitting parameters N_t, a and m. R^2 is calculated from the sum of residuals (i.e. the difference between the experimental model and model-predicted bound concentrations).

2.6. Affinity distribution (AD) analysis

Shimizu et al. [4–7] have proposed an analytical expression to calculate the ADs for those MIPs that better fit to a Freundlich isotherm:

$$N(K) = 2.303am(1 - m^2)K^{-m} \tag{7}$$

while Guiochon et al. [15,30] use a similar expression, given by the equation:

$$N(K_i) = a\frac{\sin(\pi m)}{\pi}K_i^{-m}. \tag{8}$$

Although this equation is similar to that developed by the Shimizu's group Eq. (7), the difference between them is in the approximation methods used to obtain them. Both equations have the same general mathematical form, with an identical exponentially decreasing factor ($-m$) while the pre-exponential factor is different. From any of these equations, (7) or (8), two additional binding parameters may be calculated [8,30], the number of binding sites, $N_{K_{\min}-K_{\max}}$, and the apparent average association constant, K_n:

$$N_{K_{\min}-K_{\max}} = a(1 - m^2)(K_{\min}^{-m} - K_{\max}^{-m}), \tag{9}$$

$$K_n = \left(\frac{m}{m-1}\right)\left(\frac{K_{\min}^{1-m} - K_{\max}^{1-m}}{K_{\min}^{-m} - K_{\max}^{-m}}\right). \tag{10}$$

2.7. Affinity spectrum

The isotherm equations were fit to the experimental isotherm (*Bound vs Free*) using a mathematical algorithm. The best-fit values for the isotherm parameters were obtained by varying the parameters one at a time and finding the best fit by minimizing the sum-of-squares. The goodness of fit was validated by obtaining the correlation constant values (R^2) in the range of 0.95–0.99. Standard deviations were reported as errors in the fitting isotherm parameters.

The fitting parameters were then substituted into the affinity distribution Eq. (8) and plotted in a $\ln(N(K))$ vs $\ln(K)$ format. The affinity distributions for each of the different MIPs were obtained for both CAP and CAPdi. Numbers of binding sites (N) were calculated using Eq. (8) and employing the same K_{min} and K_{max} for each MIP.

3. Results and discussion

Fig. 1 shows the amount of CAP adsorbed (B in mmol g^{-1}) vs the contact time on MIP1, MIP2 and NIP. The concentration of CAP (0.1 mM) and the amount of solids (30 mg) were kept constant along these experiments. As can be seen, the adsorption capacity, expressed as percentage uptake (ratio between the amount of CAP adsorbed and the starting concentration) is higher for the MIP1, the polymer for which it was expected more binding sites. To evaluate the specificity of the CAP imprints, the binding of CAPdi to the CAP-imprinted polymers was measured. Binding was measured but much less than was shown by CAP, consistent with the structural change in the binding molecule due to the nitro-phenyl acetamide substituent group.

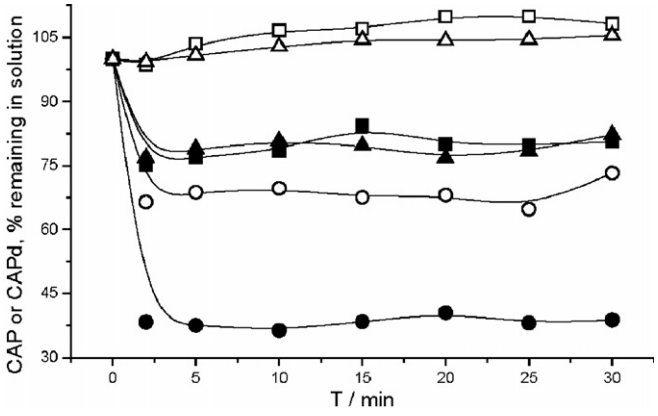

Fig. 1. Kinetics of CAP and CAPdi binding. CAP: (●) MIP1, (▲) MIP2, (■) NIP; CAPdi: (○) MIP1, (△) MIP2, (□) NIP.

The CAP and CAPdi adsorption kinetics were also investigated. The pseudo-second order kinetics equation was tested for all polymers considering the differential equation [31]:

$$d[C]/dt = k(C_e - C_t)^2, \quad (11)$$

where C_e is the amount of CAP (or CAPdi) adsorbed at equilibrium (mmol g^{-1}), C_t is the amount of CAP (or CAPdi) adsorbed at time t (mmol g^{-1}) and k is the equilibrium rate constant of pseudo-second order sorption (g $mmol^{-1}$ min^{-1}). Integrating and applying the boundary conditions $t = 0$ and $t = t$ and $C_t = 0$ and $C_t = C_t$ Eq. (11) takes the form:

$$1/(C_e - C_t) = 1/C_e + kt. \quad (12)$$

This equation may be rearranged to obtain a linear form:

$$\frac{t}{C_t} = \frac{1}{kC_e^2} + \frac{t}{C_e}. \quad (13)$$

Then, plotting of t/C_t vs t allows the kinetics parameters k and C_e to be obtained directly from the intercept and slope, respectively. In Table 1 the pseudo-second order kinetic parameters of CAP and CAP-di binding to MIP1, MIP2 and NIP are summarised. Regression coefficients, higher than 0.99, suggests that CAP and CAPdi binding to MIP1, MIP2 and NIP follows the second-order kinetic model.

These results indicate that interaction of CAP with MIP1 runned faster than with NIP or MIP2, while the interaction of CAPdi proceeded with approximately the same reaction rate whichever the polymer considered. This fact could be explained considering that the rate of target molecule adsorption to imprinted polymers is proportional to the number of collisions experienced by the template, which should be higher for CAP than for CAPdi, as it would be expected.

The binding properties of MIP1, MIP2 and NIP were determined by measuring the CAP and the CAP-di uptake over a range of concentrations, from 3×10^{-7} to 6.5×10^{-4} M. Scatchard plots were constructed for a constant mass of polymer (30 mg) and results demonstrated (Fig. 2(a) and (b)) that the plots are not linear and may be composed of two (CAP) or more (CAPdi) straight lines, thus indicating that the recognition sites in these imprinted polymers are not uniform in nature.

Table 1
Kinetic data for CAP and CAPdi binding to CAP-imprinted polymers

Polymer	Chloramphenicol			Chloramphenicol di-acetate		
	$k \times 10^{-5}$ (mg $mmol^{-1}$ min^{-1})	$C_e \times 10^6$ (mmol mg^{-1})	R^2	$k \times 10^{-5}$ (mg $mmol^{-1}$ min^{-1})	$C_e \times 10^6$ (mmol mg^{-1})	R^2
NIP	11.35	6.69	0.999	5.76	7.2	0.999
MIP1	14.55	3.23	0.997	6.56	4.6	0.990
MIP2	7.66	6.65	0.997	5.82	6.9	0.999

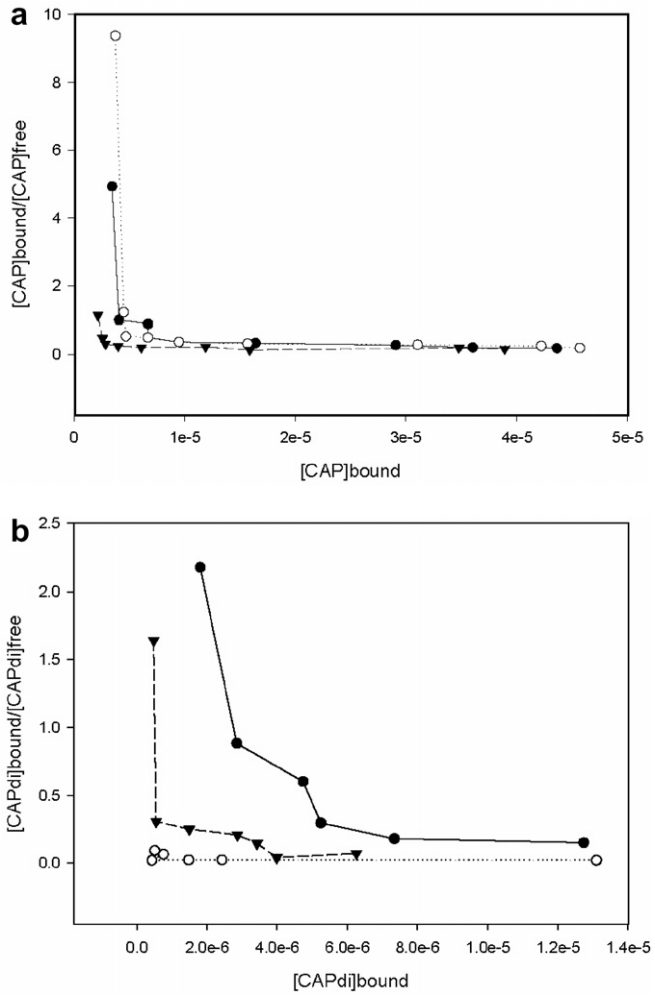

Fig. 2. Scatchard plot for CAP (a) and CAP-di (b) binding to MIP1, MIP2 and NIP. (●) MIP1; (○) MIP2; (▼) NIP.

Isotherm constants were determined by linear regression and a solver function. The adsorption isotherm parameters CAP and CAPdi with each polymer are summarised in Table 2.

As can be seen, the F and the L–F isotherms should provide a reasonable description and analysis of the experimental data for interaction of CAP with the MIP1, while for the interaction of CAPdi with both MIP1 and MIP2, the correlation coefficient was higher than 0.99 when the L–F model is considered.

The heterogeneity parameter is a measure of the ratio of high-to-low affinity sites, that is, it is a measure of the percentage of high-affinity sites. In the systems under study, the MIP1 and MIP2 showed low values of m for the binding of CAP, which indicates a higher percentage of high-affinity binding sites, as expected. Also, the MIP1 showed high-affinity binding sites for CAPdi. On the other hand, the higher values of m for the binding of CAP with NIP and that of CAPdi with MIP2 indicate more homogeneous materials with a higher percentage of low-affinity binding sites. The affinity distribution, based on the Freundlich isotherm and produced by Eq. (8) were plotted in terms of $N(K)$ vs $\ln(K)$ or $\ln(N(K))$ vs $\ln(K)$. For CAP interactions, the affinity distribution in $N(K)$ vs $\ln(K)$ format was an exponentially decreasing function. For the highest associa-

Table 2
Fitting parameters for the Langmuir, Freundlich and L–F adsorption isotherms of CAP and CAPdi binding to imprinted and control polymers

Isotherm model	m	R^2	m	R^2
	CAP-MIP-1		CAPdi-MIP-1	
L	–	0.768	–	0.943
F	0.475	0.965	0.397	0.986
L–F	0.479	0.974	0.397	0.999
	CAP-MIP-2		CAPdi-MIP-2	
L	–	0.645	–	0.667
F	0.447	0.922	0.705	0.942
L–F	0.494	0.942	0.705	0.999
	CAP-NIP		CAPdi-NIP	
L	–	0.812	–	0.803
F	0.639	0.966	0.452	0.958
L–F	0.668	0.977	0.452	0.999

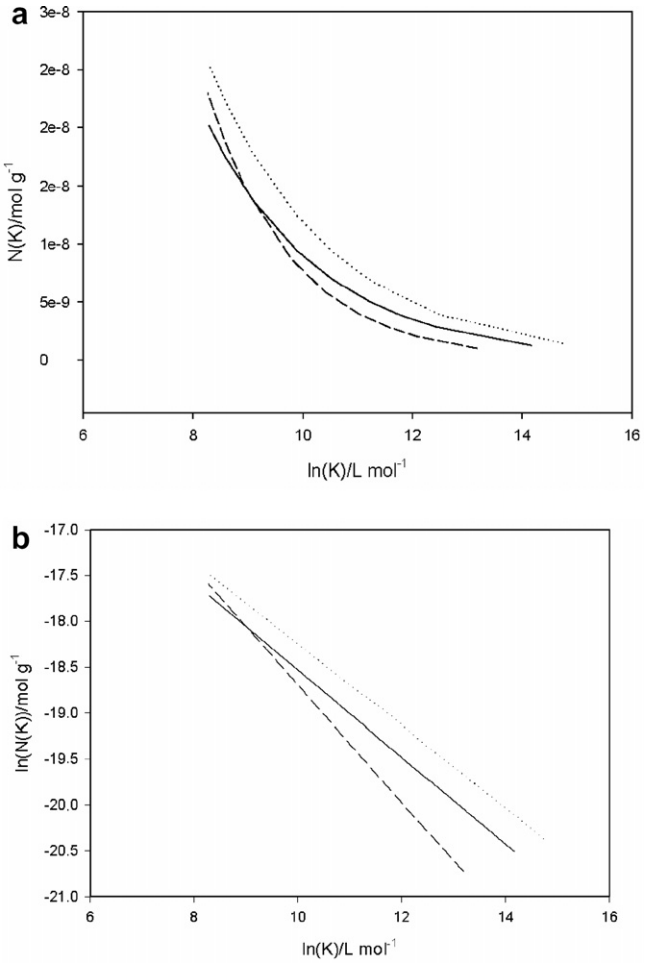

Fig. 3. Affinity distributions for CAP-binding to MIP1, MIP2 and NIP calculated using the affinity distribution function (Eq. (8)). — MIP1, …. MIP2, - - - - NIP.

Table 3
Freundlich fitting parameters, weighted average affinity and number of sites for CAP binding

Polymer	m	$a \times 10^3$ (L mol^{-1})$^{m-1}$	$K_n \times 10^{-4}$ (L mol^{-1})	$N_{K_{min}-K_{max}}$ (μmol g^{-1})	R^2
CAP-MIP1	0.475	1.9	8.1	1.8	0.965
CAP-MIP2	0.447	1.4	12	1.8	0.922
CAP-NIP	0.639	6.1	3.5	1.2	0.966

K_n and $N_{K_{min}-K_{max}}$ calculated in the range $\ln(K) = 8.3$–14.7 (L mol^{-1}).

Table 4
Freundlich fitting parameters, weighted average affinity and number of sites for CAPdi binding

Polymer	m	$a \times 10^3$ (L mol^{-1})$^{m-1}$	$K_n \times 10^{-4}$ (L mol^{-1})	$N_{K_{min}-K_{max}}$ (μmol g^{-1})	R^2
CAPdi-MIP1	0.397	0.5	14	0.5	0.986
CAPdi-MIP2	0.705	1.7	1.2	0.3	0.942
CAPdi-NIP	0.452	3.5	21	0.3	0.958

$N_{K_{min}-K_{max}}$ calculated in the range $\ln(K) = 7.3$–15.0 (L mol^{-1}).

tion constant, the affinity distribution function tends toward zero while it tends toward infinity for the lowest association constant. The format $\ln(N(K))$ vs $\ln(K)$ generates straight lines. Visual inspection on vertical positions and slopes of the affinity distributions allows to compare quality of binding sites among affinity distributions generated by the different MIPs against the two target molecules, CAP and CAPdi. Fig. 3 shows the affinity distributions generated by CAP with polymers MIP1, MIP2 and NIP and in Table 3 the corresponding Freundlich fitting parameters.

As can be seen, MIP1 and MIP2 have similar capacities (number of binding sites) and similar ratio of high-to-low-affinity sites. However, MIP2 showed a weighted average affinity constant that was two-fold that of MIP1. These results indicate that it is possible to reduce the template concentration by more than a factor of 10 without significant loss of the recognition properties. Compared to MIP1 and to MIP2, NIP has a lower capacity, a lower percentage of high-affinity binding sites and a lower average affinity constant.

In Table 4 the affinity distribution parameters obtained using Freundlich isotherm for the CAPdi system are summarized. Again, the affinity distribution in $N(K)$ vs $\ln(K)$ format was an exponentially decreasing function for the CAPdi system while the format $\ln(N(K))$ vs $\ln(K)$ generated straight lines. In this case, the MIP1 and the NIP exhibited different capacity but a similar ratio of high-to-low affinity binding sites. Compared to MIP1, the MIP2 showed lower capacity, lower percentage of high-affinity binding sites against CAPdi and a lower average affinity constant.

Based on above results, it is interesting to observe that the MIP2, prepared in the presence of a lower amount of CAP, showed enhanced affinity properties for CAP than for CAPdi while the affinity properties were reversed when dealing with the MIP1, the polymer prepared with a higher concentration of CAP. This emphasises the importance of the template concentration during the polymer preparation when tailoring selective molecularly imprinted polymers.

4. Conclusions

This work has demonstrated that the affinity distribution analysis combined with the Freundlich binding model allowed to characterize the binding properties of two imprinted polymers for CAP prepared in presence of different amount of the template. Results demonstrated the importance of the amount of template during polymer preparation for tuning the selectivity and the affinity of the binding process. Also, kinetic data demonstrated that the rate of template adsorption to imprinted polymers was proportional to the number of collisions experienced by the template, which should be higher for CAP than for CAPdi, as it would be expected since the polymers were imprinted with CAP.

Acknowledgements

Authors gratefully acknowledge MCYT (Project # MCT-03-BQU-00853) for financial support. E.Corton acknowledges Oviedo University (Spain) and Buenos Aires University (Argentina) for support (Research Agreement).

References

[1] B.J. Stanley, P. Szabelski, Y.B. Chen, B. Sellergren, G. Guiochon, Langmuir 19 (2003) 772.
[2] F. Lanza, M. Rüther, A.J. Hall, C. Dauwe, B. Sellergren, Mat. Res. Soc. Symp. Proc. vol. 723, Publisher by Materials Research Society, 2002, p. 93.
[3] R.J. Umpleby II, M. Bode, K.D. Shimizu, Analyst 125 (2000) 1261.
[4] R.J. Umpleby II, S.C. Baxter, M. Bode, J.K. Berch Jr., R.N. Shah, K.D. Shimizu, Anal. Chim. Acta 435 (2001) 35.
[5] R.J. Umpleby II, S.C. Baxter, Y. Chen, R.N. Shah, K.D. Shimizu, Anal. Chem. 73 (2001) 4584.

[6] T. Takeuchi, T. Mukawa, J. Matsui, M. Higashi, K.D. Shimizu, Anal. Chem. 73 (2001) 3869.
[7] A.M. Rampey, R.J. Umpleby II, G.T. Rushton, J.C. Iseman, R.N. Shah, K.D. Shimizu, Anal. Chem. 76 (2004) 1123.
[8] R.J. Umpleby II, S.C. Baxter, A.M. Rampey, G.T. Rushton, Y. Chen, K.D. Shimizu, J. Chromatogr. B 804 (2004) 141.
[9] G.T. Rushton, C.L. Karns, K.D. Shimizu, Anal. Chim. Acta 528 (2005) 107.
[10] P. Sajonz, M. Kele, G. Zhong, B. Sellergren, G. Guiochon, J. Chromatogr. A 810 (1998) 1.
[11] Y. Chen, M. Kele, P. Sajonz, B. Sellergren, G. Guiochon, Anal. Chem. 71 (1999) 928.
[12] I. Quiñones, A. Cavazzini, G. Guiochon, J. Chromatogr. A 877 (2000) 1.
[13] K. Miyabe, G. Guiochon, Anal. Sci. 16 (2000) 719.
[14] Y. Chen, M. Kele, I. Quiñones, B. Sellergren, G. Guiochon, J. Chromatogr. A 927 (2001) 1.
[15] P. Szabelski, K. Kaczmarski, A. Cavazzini, Y.-B. Chen, B. Sellergren, G. Guiochon, J. Chromatogr. A 964 (2002) 99.
[16] P. Szabelski, G. Götmar, D. Zhou, B.J. Stanley, G. Guiochon, Anal. Chem. 76 (2004) 197.
[17] H. Kim, K. Kaczmarski, G. Guiochon, Chem. Eng. Sci. 60 (2005) 5425.
[18] H. Kim, G. Guiochon, J. Chromatogr. A 1097 (2005) 84.
[19] F. Gritti, G. Guiochon, J. Chromatogr. A 1097 (2005) 98.
[20] H. Kim, G. Guiochon, Anal. Chem. 77 (2005) 93.
[21] H. Kim, G. Guiochon, Anal. Chem. 77 (2005) 1708.
[22] H. Kim, G. Guiochon, Anal. Chem. 77 (2005) 1718.
[23] H. Kim, G. Guiochon, Anal. Chem. 77 (2005) 2496.
[24] H. Kim, G. Guiochon, Anal. Chem. 77 (2005) 6415.
[25] H. Kim, K. Kaczmarski, G. Guiochon, J. Chromatogr. A 1101 (2006) 136.
[26] H. Kim, K. Kaczmarski, G. Guiochon, Chem. Eng. Sci. 61 (2006) 1122.
[27] J.L. Suárez Rodríguez, M.E. Díaz-García, Biosens. Bioelec. 16 (2001) 955.
[28] R. Sips, J. Chem. Phys. 16 (1948) 490.
[29] R. Sips, J. Chem. Phys. 18 (1950) 1024.
[30] D.A. Spivak, Adv. Drug Deliver. Rev. 57 (2005) 1779.
[31] G. Crini, H.N. Peindy, Dyes Pigments 70 (2006) 204.